

Roles of I_A and morphology in action potential propagation in CA1 pyramidal cell dendrites

Corey D. Acker · John A. White

Received: 4 July 2006 / Revised: 21 January 2007 / Accepted: 8 March 2007 / Published online: 20 April 2007
© Springer Science + Business Media, LLC 2007

Abstract Dendrites of CA1 pyramidal cells of the hippocampus, along with those of a wide range of other cell types, support active backpropagation of axonal action potentials. Consistent with previous work, recent experiments demonstrating that properties of synaptic plasticity are different for distal synapses, suggest an important functional role of bAPs, which are known to be prone to failure in distal locations. Using conductance-based models of CA1 pyramidal cells, we show that underlying “traveling wave attractors” control action potential propagation in the apical dendrites. By computing these attractors, we dissect and quantify the effects of I_A channels and dendritic morphology on bAP amplitudes. We find that non-uniform activation properties of I_A can lead to backpropagation failure similar to that observed experimentally in these cells. Amplitude of forward propagation of dendritic spikes also depends strongly on the activation dynamics of I_A . I_A channel properties also influence transients at dendritic

branch points and whether or not propagation failure results. The branching pattern in the distal apical dendrites, combined with I_A channel properties in this region, ensure propagation failure in the apical tuft for a large range of I_A conductance densities. At the same time, these same properties ensure failure of forward propagating dendritic spikes initiated in the distal tuft in the absence of some form of cooperativity of synaptic activation.

Keywords Backpropagation · Propagation failure · Traveling wave attractor · bAP · Dendritic spike

1 Introduction

Backpropagation of axonal action potentials into the dendritic arbor is supported by a wide variety of neurons and is thought to play an important role in several cellular functions, including synaptic integration, and synaptic plasticity (Häusser et al. 2000; Stuart and Häusser 2001; Johnston et al. 2003; Gullidge et al. 2005). In spike-timing-dependent plasticity (STDP) protocols, pairings with a short delay between the synaptic input and a postsynaptic action potential usually lead to long term synaptic potentiation (Magee and Johnston 1997; Markram et al. 1997; Bi and Poo 1998). This potentiation is thought to depend primarily on depolarization-induced unblocking of NMDA channels and supralinear NMDA calcium influx. It was recently discovered that STDP when observed at distal synapses, is significantly different than when observed at proximal synapses (Froemke et al. 2005; Sjöström and Häusser 2006).

These new findings are consistent with the hypothesis that backpropagating action potentials (bAPs) play an important role in the STDP phenomenon providing the necessary depolarization for potentiation. It is well known

Electronic supplementary material The online version of this article (doi:10.1007/s10827-007-0028-8) contains supplementary material, which is available to authorized users.

Action Editor: Alain Destexhe

C. D. Acker (✉)
Department of Neuroscience,
University of Connecticut Health Center,
263 Farmington Avenue, Farmington, CT 06030, USA
e-mail: acker@uhc.edu

J. A. White
Department of Biomedical Engineering, Boston University,
44 Cummington St., Boston, MA 02215, USA

C. D. Acker · J. A. White
Department of Biomedical Engineering,
Center for BioDynamics, and Center for Memory and Brain,
Boston University, Boston, MA, USA

that bAPs propagate decrementally in dendrites of many cell types including apical dendrites of cortical and hippocampal pyramidal neurons (Stuart and Sakmann 1994; Spruston et al. 1995). Decreased action potential amplitude at distal synapses leads to decreased NMDA calcium influx when paired with synaptic stimulation, which can explain the weakened potentiation observed experimentally (Froemke et al. 2005). At far distal synapses, pairings that normally produce potentiation, have been observed to produce depression instead (Sjöström and Häusser 2006). This dramatic change in plasticity may be explained by considering action potential failure at these distal regions, which would lead to dramatically reduced calcium entry.

The properties of backpropagating action potentials (bAPs), including their amplitudes and widths, likely impact the roles that they play. In some CA1 pyramidal cells, bAPs decline initially and then fail (Golding et al. 2001). Failures are of particular interest because, as recently demonstrated in physiologically similar cortical pyramidal cells (Sjöström and Häusser 2006), they may cause dramatic changes in cellular function such as a switch from synaptic potentiation to depression. Our goal is to better understand the biophysical properties of dendrites that control the decline and failure of bAPs. It has been demonstrated that both voltage-gated channel properties and morphological properties can contribute to bAP decline and failure (Golding et al. 2001; Vetter et al. 2001). In CA1 pyramidal cells, blocking I_A blocks the decline in amplitude normally exhibited (Hoffman et al. 1997), and models show that altering the distribution of I_A can determine whether or not bAPs reach the end of the dendrite (Migliore et al. 1999; Golding et al. 2001). In some circumstances, dendritic branching also contributes to the apparent failure of bAPs in these models (Golding et al. 2001).

In this work, we compare generation and propagation of APs in simple cable models with that in a morphologically complex model of apical dendrites of CA1 pyramidal cells. In each case we can compute traveling wave attractors at every location along the cable or model dendrite. These attractors reveal what the propagating action potential would look like if it were propagating in a long dendrite with uniform properties. This method allows one to quantitatively and independently study effects due to channel properties and branching. Since these attractors do not depend on propagation direction, the same attractor applies to both backpropagating action potentials and forward propagating dendritic spikes, and the effects of channel properties are investigated in both cases.

Increasing I_A conductance density with distance from the soma along CA1 apical dendrites, along with changing channel kinetics, leads to declining backpropagating action potential amplitude with distance. The rate of decline can be accurately predicted along with the critical location at

which channel properties no longer support regenerative propagation and beyond which propagation failure occurs. Before the I_A conductance density is sufficient to block active propagation, a non-robust action potential is supported that is sensitive to perturbations due to dendritic branching. The conditions that result in propagation failure at branch points are computed, which for the CA1 model considered ensure propagation failure in the distal tuft for a range of I_A distributions, as well as failure of forward propagating dendritic spikes initiated in the distal tuft in the absence of some form of cooperativity of synaptic activation.

2 Materials and methods

2.1 CA1 pyramidal cell models

The computational models of apical dendrites of CA1 pyramidal cells used here are based on previously published models (Migliore et al. 1999). Dendritic morphology is manipulated extensively and action potential propagation in simplified, surrogate morphologies is compared to that in the previously published detailed model. In Fig. 1, a perfectly uniform cable model is used to demonstrate the relevance of traveling waves (described below) in these models. Subsequently, a branchless “ball-and-stick” morphology is considered consisting of a soma coupled to a single long dendrite section (Fig. 3(a)). A single compartment, cylindrical soma section is used with length and diameter equal to 11.6 μm so that the surface area matches that in the original model. The dendrite is 600 μm in length and has a constant diameter equal to 1.8 μm . This is an intermediate diameter, considerably smaller than the large initial apical diameter, but considerably larger than the fine distal apical dendritic segments. Effects due to branching in apical dendrites are subsequently studied using the originally published, morphologically detailed CA1 pyramidal cell model (Migliore et al. 1999) with the axon and basal dendrites omitted (Fig. 7(a)).

Voltage-gated ionic currents, their space-dependent distributions and dynamics are modeled based closely on previously published models (Migliore et al. 1999). Fast sodium (I_{Na}), delayed rectifier potassium (I_{KDR}), and A-type potassium (I_A) currents, crucial in controlling backpropagation, are included. I_{Na} and I_{KDR} are distributed uniformly, i.e. constant conductance density over the length of the dendrite. I_A is distributed non-uniformly; the channel density increases linearly as a function of distance from soma. Channel activation dynamics are also space-dependent. The activation curve for distally situated I_A channels is hyperpolarization-shifted by approximately 10mV, mimicking experimental observations (Hoffman et al. 1997). Changes in I_A channel inactivation observed in response to protein kinase activity

(Hoffman and Johnston 1998) are not included in this model. While we do not address the implications of modulation of channel inactivation, it is important to mention that these effects tend to oppose those due to changes in channel activation, but are significantly weaker. In this model, the time constant of I_A channel activation is approximately double for proximally situated channels compared to distally situated ones. While this effect has not been published experimentally, it is consistent with changes in channel activation rate constants that lead to a hyperpolarization-shifted activation curve at distal dendrites (Hoffman et al. 1997).

The consequences of space-dependent I_A channel distribution and channel activation properties are studied independently by separating them as follows. Space-dependent changes in channel dynamics are removed by taking a weighted average of voltage-dependent equations (Eq. (1)). The resulting averaged dynamics are then applied uniformly to the entire dendrite and channel distribution can be varied independently.

$$F_{\text{avg}}(V_m) = W \cdot F_{\text{prox}}(V_m) + (1 - W) \cdot F_{\text{dist}}(V_m) \quad (1)$$

W , the weight value between 0 and 1, is chosen to be 0.1 (predominantly “distal” I_A activation dynamics, Fig. 3) and is applied to both the steady state equations and time constant equations for I_A activation. Alternatively, by holding the distribution of I_A fixed, the effects on propagation due to the variations in I_A activation properties can be studied (Figs. 4, 5).

2.2 Multicompartmental simulations

Multicompartmental simulations are performed using MNeuron, custom software written in MATLAB (for more information, contact the author C. Acker). MNeuron takes advantage of MATLAB’s numerical integrator of sparse, stiff systems of ODEs, ode15s. By default, the relative error tolerance is 10^{-7} and the absolute error tolerance is 10^{-6} . MATLAB graphical user interfaces are used extensively, while equations for membrane conductances are modular, and can be compiled for improved simulation speed. Intercompartmental coupling strengths for tapering dendrites are calculated as in the literature (Eq. (6.30), Pg. 220, Dayan and Abbott 2001). For the simple cable model, the 600 μm length dendrite is divided into 80 equally spaced, 7.5 μm length compartments. For the morphologically detailed model (Fig. 7), each dendritic segment is divided into the minimum number of equal length compartments such that they have a maximum length of 7.5 μm . This spatial discretization is adequate for the models presented here because only small, quantitative differences appear when the maximum compartment size is doubled to 15 μm (data not shown).

2.3 Traveling wave attractors

In uniform dendrites or axons, action potential propagation may be stable. If so, action potentials propagate as traveling waves: with fixed waveform and constant velocity. This steady propagation corresponds to a time-dependent stable state; small perturbations lead to changes in waveform that decay over time, leaving only a time or position shift with respect to the unperturbed waveform. We refer to this stable state as a *traveling wave attractor*, with *attractor* for our purposes referring to the fact that the state is stable, i.e. attracting. Computing traveling wave attractors is done using the same strategy as in classical papers on action potential propagation in axons (Hodgkin and Huxley 1952). The nonlinear cable equation (partial differential equation) is transformed to a set of ordinary differential equations (ODEs) by assuming the existence of a traveling wave solution where all variables depend on space and time as follows: $y(x, t) = y(x - ct)$ (see Section 4.3, pg. 200, Weiss 1996), where c is the wave speed given by:

$$c = \sqrt{\frac{K \cdot d}{4 \cdot \text{Ra} \cdot C_m}} \quad (2)$$

d is the cable diameter, Ra is the intracellular resistivity, and C_m is the membrane capacitance. The value of K depends on the voltage-gated channel properties. After the transformation, the system of ODEs, the traveling wave equations, is analyzed in XPPAUT (Ermentrout 2002, still unavailable in 1952). The correct value of the parameter K is found using a trial-and-error method called *shooting* in which a homoclinic orbit corresponding to a stable traveling wave is sought. When such an orbit can be found, K is determined to four significant digits, and is recorded along with the amplitude of the resulting traveling wave waveform, and the wave speed calculated using Eq. (2). Since the homoclinic orbit found can correspond to a stable or unstable traveling wave, simulations of the full cable equations are used to confirm stability. A tutorial for computing traveling wave attractors in XPPAUT, along with the necessary code and model equations, is available as supplemental material.

For nonuniform dendrite models, one does not expect a traveling wave with unchanging waveform. The expected changes in waveform are in fact what we are interested in. However, we proceed by treating each compartment in the model as if it were an infinitely long cable with uniform properties. All the properties from each compartment in the model dendrite (maximal conductances, reversal potentials, etc.) are loaded into XPPAUT along with the dynamic equations. The resulting “local” traveling wave attractor corresponding to each set of “local” properties is then computed as described above. In addition to the local

properties mentioned above, a constant current is applied so that the rest state exactly matches the resting state of the local dendrite compartment. This adjustment is important to account for non-uniform resting potentials that can arise in models with non-uniform channel properties. The current applied matches the net current flowing into the specific compartment from neighboring compartments when the model is at rest ($\frac{\partial v}{\partial t} = 0$, for all variables).

Parameters are transferred automatically from MATLAB to XPPAUT by a Python script that modifies the XPPAUT.ode file. Two methods are used to confirm that parameters are transferred correctly and that results from the multi-compartmental simulations (MATLAB) are consistent with simulations of the traveling wave equations (XPPAUT). First, resting potentials are compared between the two programs and never differ by more than 3 μV . Second, traveling wave waveforms found in XPPAUT are compared to those recorded from multicompartmental simulations of a uniform dendrite with matching membrane properties/parameters. In Fig. 1, one can see that the resulting waveforms are very similar, indicating very good correspondence between the two different numerical methods used in this example. In our experience with these comparisons, the peak action potential amplitudes found are not as precise as the resting potentials but have never differed by more than 0.5 mV.

3 Results

3.1 Traveling waves in a uniform cable model of a CA1 pyramidal cell dendrite

Action potential propagation in neuronal dendrites can exhibit variations in waveform, such as changes in amplitude, including distinct drop-offs in amplitude referred to as propagation failures (Golding et al. 2001). These waveform changes result from the non-uniform properties of dendrites including non-uniformly distributed voltage-gated ion channels (Migliore et al. 1999; Golding et al. 2001), and morphological features such as branching (Goldstein and Rall 1974; Manor et al. 1991). While our goal is to better understand the complex propagation in these nonuniform structures, it is informative to first study propagation in simplified models with these non-uniformities removed.

In a uniform cable model of a CA1 pyramidal cell apical dendrite, action potentials quickly approach steady-state propagation after a brief initial transient (Fig. 1). While this model has a finite length, it is useful to remember that in infinitely long, uniform cables, steady state propagation corresponds to a traveling wave with a fixed waveform and constant propagation velocity. In reality, one finds that the uniform cable model need not be very long to approximate

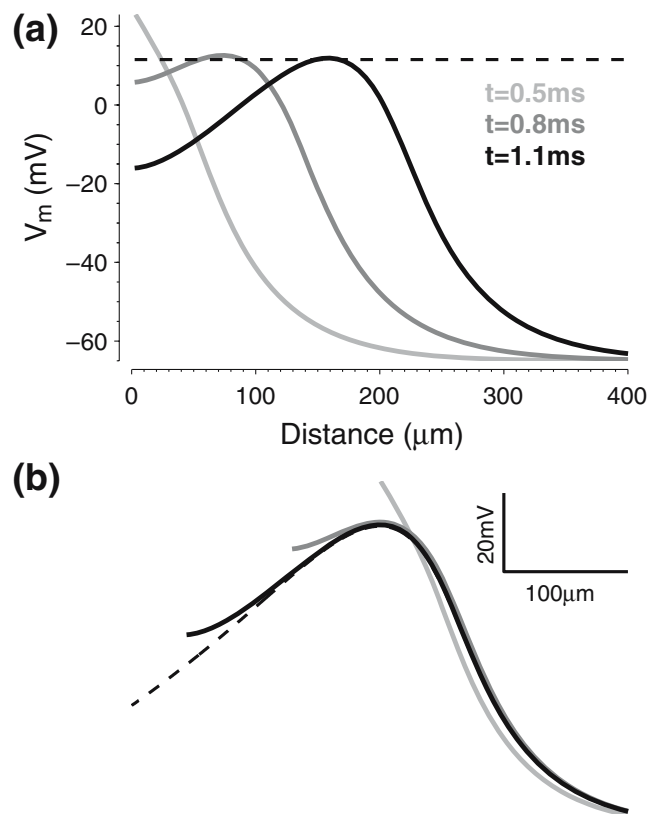


Fig. 1 In a uniform dendrite model, a backpropagating action potential quickly becomes a traveling wave after a brief initial transient. **(a)** A current pulse (1.0 nA, 0.5 ms) is applied to first dendritic compartment to elicit the action potential. Time snapshots at 0.5, 0.8, and 1.1 ms after onset of pulse are shown. *Grayscale shades of lines match inset legend text. Dashed line is peak amplitude of traveling wave attractor of this model (see panel (b)).* Model parameters as in Fig. 3(c), *light gray*, except dendrite length is 1,200 μm (only first 400 μm shown), and soma is excluded. Steady-state membrane potential is -65 mV. **(b)** Traveling wave attractor for this model computed as described in Section 2 (*dashed line*, wave speed=0.274 m/s) along with three time snapshots of bAP from panel (a) (*solid lines*), plotted with their peaks aligned

an infinite cable. Instead, the propagating action potential quickly approaches the traveling wave expected in the infinite version (computed as described in Section 2).

The observed propagation behavior can be described as a system approaching its stable state, which in this case is a traveling wave. Since this state is stable, i.e. attracting, we refer to it as the traveling wave *attractor*. The “attractiveness” of this stable state would refer to the rate at which it is approached (for limit cycles, this rate can be computed using Floquet multipliers, Acker et al. 2003). In this model, the action potential’s amplitude is near its steady-state value after the peak of the wave has advanced approximately 150 μm . Since the model is much longer than 150 μm , the attractiveness of the stable state is sufficiently strong such that this model may be considered an infinitely long uniform cable. The concept of attractiveness will be important when

later we study propagation behavior in non-uniform dendrites. It should be mentioned that this model is bistable; rest is also a stable state, which is why a pulse of current is necessary to trigger the propagating action potential behavior.

3.2 Action potential sensitivity to I_A conductance and action potential failures

It has been demonstrated previously that blocking I_A channels pharmacologically in CA1 pyramidal neurons leads to increased amplitudes of backpropagating action potentials (Hoffman et al. 1997). While this effect is intuitive, it is important to quantitatively study this relationship between channel conductance density and action potential propagation. This can be done by computing traveling wave stable states while varying the channel property of interest. This analysis reveals how smooth

changes in channel properties can cause abrupt changes in propagation behavior, such as propagation failure similar to that seen experimentally, when there is a change in the system’s stable states.

By computing traveling wave attractors, we compute the sensitivity of action potential amplitude to I_A channel conductance density (Fig. 2). The same model is used as in Fig. 1 except that the model’s maximal I_A conductance, g_{KA} , is varied. As expected, increasing g_{KA} leads to decreasing peak amplitudes of the propagating action potential. At the published value of g_{KA} (48 mS/cm², the model’s set point in this analysis), the slope of this curve, the instantaneous sensitivity to g_{KA} , is -0.3 mV/mS/cm². In a non-uniform dendrite model with varying I_A conductance density, changes in action potential amplitude can be expected to reflect this sensitivity. When g_{KA} increases past 190 mS/cm² in this model, there is a sudden change in the system’s steady state: the traveling wave attractor disappears and the propagating action potential is no longer a stable state. A sudden change in the number or nature of a system’s stable states is known as a bifurcation. In this case, the (stable) traveling attractor disappears before reaching zero amplitude, which indicates annihilation by merging with an (unstable) traveling wave repeller. This bifurcation leaves the rest state as the only remaining stable state without the possibility of sustained action potential propagation.

3.3 I_A distribution controls backpropagation amplitude in a branchless model and can lead to propagation failure

Experimentally it has been shown that in some neurons, backpropagating action potentials can fail at a certain location along the dendrite (Golding et al. 2001). Since the distributions and properties of voltage-gated ion channels are thought to vary fairly smoothly along the length of the dendrites, it may seem unlikely that channel properties play a role in these failures. For the same reasons, branch points may seem much better candidates since they exist at distinct locations, and one of these locations might correspond to the location at which propagation fails. However, using reconstructions of neurons, a clear “responsible” branch point was not found (Golding et al. 2001). Here, we use a branchless model and show how non-uniform channel properties can lead to backpropagation behavior, including backpropagation failure, that mimics that seen in experiments.

In a “ball-and-stick” model including a soma and a single section of constant diameter apical dendrite, backpropagation is observed for three distributions of I_A (Fig. 3, panel (b) shows I_A distributions). One of the distributions is the uniform distribution considered previously (Fig. 1)

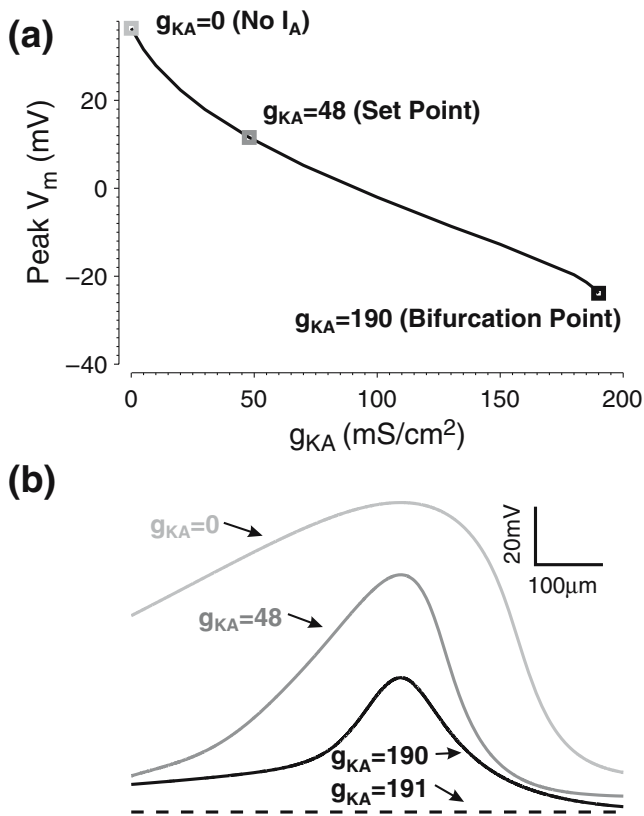


Fig. 2 Smooth increases in maximal I_A conductance can lead to abrupt failure of action potential propagation. **(a)** Peak amplitudes of the model’s steady-state action potential waveforms (traveling wave attractors) are plotted as a function of maximal I_A conductance, g_{KA} (mS/cm²). No traveling wave attractor exists when g_{KA} is greater than 190 (failure, or bifurcation point), i.e. the model does not support a propagating action potential. **(b)** Traveling wave attractors for values of g_{KA} , for which attractors exist (solid lines). Dashed line is the steady-state membrane potential for $g_{KA}=191$ mS/cm²

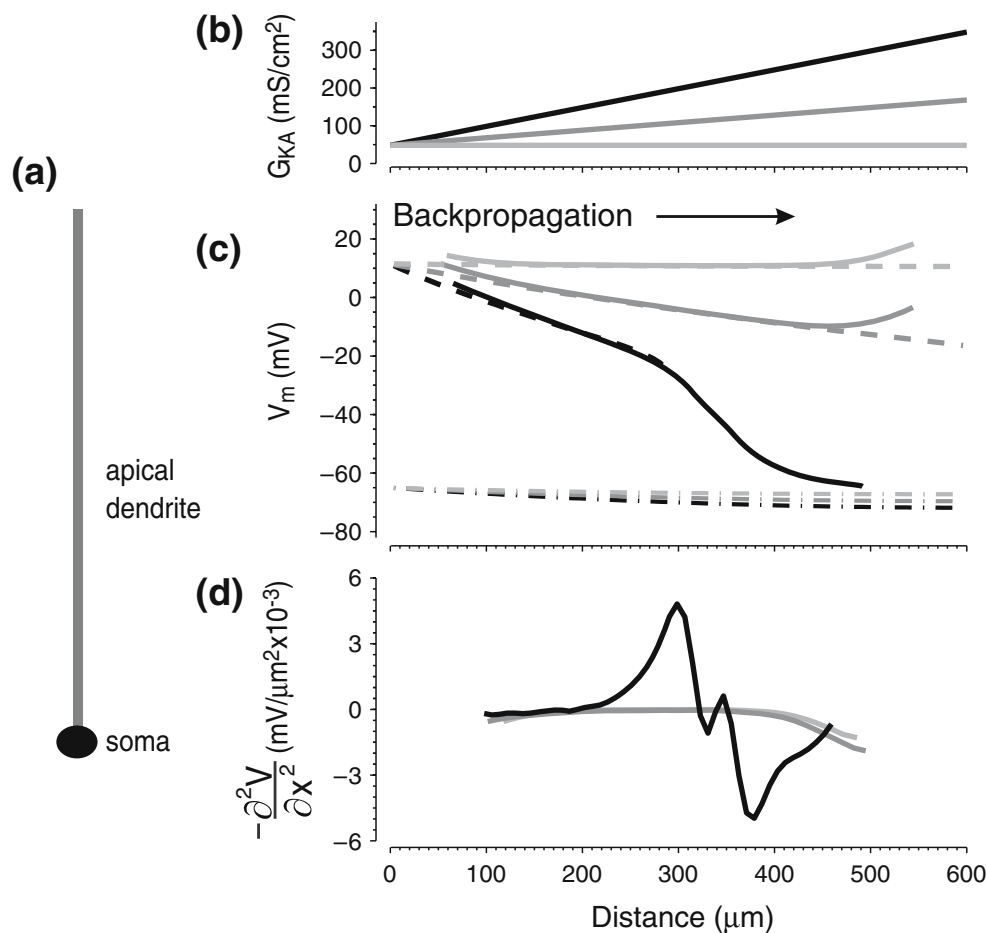


Fig. 3 Backpropagation amplitude in a ball-and-stick CA1 pyramidal cell model: the effects of non-uniformly distributed I_A conductance. Voltage-gated ion channel distributions and dynamics are as published previously for CA1 pyramidal cells (Migliore et al. 1999). **(a)** Cartoon of model neuron (not to scale). Soma is coupled to the apical dendrite, modeled as a 600 μm long branchless cable with a constant diameter of 1.8 μm (see Section 2). **(b)** Three distributions of I_A are compared. G_{KA} , the maximal conductance density (mS/cm^2), is plotted as a function of distance from soma for the three cases. G_{KA} increases in density with a

slope of 0, 0.2, or 0.5 ($\text{mS}/\text{cm}^2/\mu\text{m}$, light gray, dark gray, and black lines, respectively). **(c)** Backpropagating action potentials (bAPs) are triggered at the model's soma using a brief current pulse. The peak amplitude of each bAP is calculated every 50 μs and plotted as a function of distance from the model's soma (solid lines). Gray scale shades correspond to the I_A distributions in panel **(b)**. Dashed-dotted lines indicate resting membrane potentials. **(d)** Negative of second spatial derivative of peak amplitude data from panel **(c)**. Amplitude data are first resampled to a uniform grid and results are filtered using a Hamming window

while the other two show increasing densities with distance from soma. The peak amplitude of the propagating action potential, triggered by a brief somatic current pulse, is calculated every 0.05 ms and plotted as a function of distance from the soma (Fig. 3(c), solid lines). Two important qualitative features of backpropagation amplitude are apparent that match experimentally observed backpropagation amplitude in these cells. First, the amplitude of the backpropagating action potential tends to decrease as a function of distance from the cell soma (Johnston et al. 1999; Golding et al. 2001). Second, backpropagation can apparently fail, i.e. the AP amplitude can drop off quickly with distance beyond a specific dendritic location (Golding et al. 2001). This change in slope (Fig. 3(c), black line)

becomes obvious when the negative second derivative of these peak voltage data are computed (Fig. 3(d)).

3.4 Local traveling wave attractors predict backpropagation behavior and role of I_A distribution

For each of the three dendrite models with differing distributions of I_A (Fig. 3(c)), traveling wave attractors can be calculated for each compartment in the multicompartmental model. As described in Section 2, each compartment is assumed to be an infinite cable with uniform properties and steady-state traveling waves are computed for each compartment. When the peak amplitudes of these traveling wave attractors (Fig. 3(c), dashed lines) are compared to the

peak amplitudes of simulated backpropagating action potentials (Fig. 3(c), solid lines), one can see that they are typically very similar. The differences near the soma are due to the same transient decrease in action potential amplitude seen previously in the hypothetical uniform cable dendrite model (Fig. 1). These transients disappear within the first 200 μm , and subsequently, the bAP amplitudes track the attractors very closely, indicating that the attractors are controlling the propagation behavior.

In the cases of nonuniform I_A distribution it is clear that the traveling wave attractor is sensitive to the shifting channel conductances. In the models with increasing I_A conductance density, the attractor amplitudes decrease nearly linearly with distance from the soma and the slope of this decline depends on the slope of the increase in I_A conductance. In the uniform model (light gray), the attractor amplitude remains constant for the length of the dendrite. In the other two cases with rising I_A conductance, traveling wave attractor amplitudes fall with distance with slopes of -0.04 and -0.12 mV/ μm for the intermediate and steepest cases (dark gray and black dashed lines, respectively). After the initial transients, backpropagating action potentials follow these underlying attractors very closely, falling in amplitude with similar slopes. This close correspondence indicates that the backpropagating action potential is closely tracking a slowly changing steady state, given by the traveling wave attractors. Thus, the change in membrane properties can be considered “adiabatic.” It is important to keep in mind that for more abrupt, non-adiabatic changes in I_A channel density than those considered in Fig. 3, it may not be possible for the propagating action potential to track the changing underlying steady state, and that discrepancies between simulations and traveling wave attractors may arise. Abrupt features such as boundaries, step-wise changes in channel kinetics, and branch points can never be considered to be adiabatic changes and instead lead to transients that can be measured by comparing simulations to traveling wave attractors or simulations that do not include the studied non-adiabatic change in parameters.

Transients in action potential amplitude can be observed at the dendrite tip depending on I_A channel distribution (Fig. 3(c)). In the two cases in which the backpropagating action potential still has significant amplitude near the end of the dendrite, there is a transient increase in action potential amplitude. These rises in amplitude are due to the interactions of the propagating waves with the sealed boundary at the end of the dendrite, shown previously to cause a transient increase in amplitude (Goldstein and Rall 1974). Notice that the traveling wave attractor does not deviate near the boundaries of the model dendrite. Even these terminal compartments are assumed to be infinite

cables in order to compute the travel wave attractors. This useful property of traveling wave attractors allows one to quickly quantify the effects of the sealed dendrite tip. Since the attractors predict propagation behavior very accurately in the absence of any abrupt change in morphology such as a sealed tip, any discrepancy between the simulated action potential and the attractor is attributable to the change in morphology. Later, this strategy will be used to dissect the effects of dendritic branching from the effects of voltage-gated ion channels (Fig. 7).

In the case of steepest I_A conductance density (Fig. 3, black lines), backpropagation seems to fail near 300 μm as indicated by the large drop in the rate of decrease of peak amplitude with distance (Fig. 3(d)). In this case the traveling wave attractor disappears near 300 μm in exactly the same way that the attractor disappears when g_{KA} is increased sufficiently in uniform models (Fig. 2). This sudden disappearance of the underlying traveling wave causes the dramatic change in backpropagation in the absence of any changes in dendritic morphology and as mentioned, the location of attractor failure is a very good predictor of the location of action potential failure. This explains how non-uniform, but smooth channel distributions alone, in the absence of any critical branch point can lead to abrupt decline in action potential amplitude as observed experimentally (Golding et al. 2001).

3.5 Distance-dependent changes in I_A channel dynamics have dramatic effects on backpropagation amplitude

In Fig. 3 we showed, as other groups have shown (Migliore et al. 1999; Golding et al. 2001), that the distribution of I_A has a significant impact on bAPs in model CA1 pyramidal cells. Increasing I_A density decreases bAP amplitude and can cause backpropagation failure. These effects on backpropagation can be accurately predicted by the underlying traveling wave attractors. Next, we show how changes in I_A channel kinetics, independent of distribution, can dramatically affect backpropagation amplitude.

Dynamic properties of I_A change considerably when measured near the soma compared to when measured far from the soma in CA1 pyramidal cells (Hoffman et al. 1997). These two “types” of I_A that have been observed on proximal and distal apical dendrites differ significantly in two ways. First, I_A recorded more than 100 μm from the soma activates at lower voltages (by approximately 10 mV) compared with that recorded proximal to the soma (Hoffman et al. 1997; Migliore et al. 1999). Second, I_A in the distal dendrite activates approximately twice as rapidly as that recorded proximally (Hoffman et al. 1997; Migliore et al. 1999; see Section 2). Qualitatively, both of these differences allow distal I_A channels to react more rapidly to

upswings in potential during action potential onset. We therefore refer to the I_A dynamics observed distally as “fast” and proximally as “slow.”

3.6 “Fast” I_A limits backpropagation amplitude and promotes backpropagation failure

In order to study the effects on propagation of the two different types of I_A dynamics observed in CA1 pyramidal cell, we study two dendrite models, one with “fast” and one with “slow” I_A (equations from Migliore et al. 1999). For these simulations, the distribution of I_A is the same in both cases and matches the black lines in Fig. 3. For the “slow” form of I_A , the traveling wave attractor predicts that the action potential amplitude should decrease by 5.3 mV every 100 μm (Fig. 4, black dashed line, slope = 53 mV/mm). In the corresponding multi-compartmental simulation (solid black), we see that this is an accurate prediction away from the boundaries. Backpropagation behavior changes significantly when the “fast” form of I_A is incorporated in the model dendrite. In this case, the action potential is expected to have smaller amplitude initially, to decrease more rapidly with distance (12 mV every 100 μm), and to fail to backpropagate at a distance of 245 μm (gray dashed line). Again, multi-compartmental simulations confirm these predictions; the action potential follows the attractor closely and declines significantly more rapidly after 250 μm (solid gray).

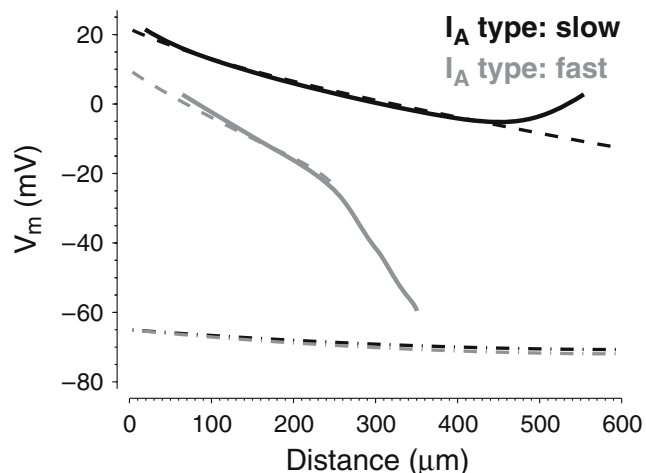


Fig. 4 Effects of activation properties of I_A on backpropagating action potential amplitude. Two identical dendrite models are compared except that in one case I_A is of the “slow reacting” type (found on proximal dendrites, *black lines*), while in the other case I_A is of the “fast reacting” type (found on distal dendrites, *gray lines*). Amplitude of the action potential is plotted for the two cases (*solid lines*) along with amplitude of the traveling wave attractors (*dashed lines*). When the model includes the fast reacting version of I_A , the traveling wave attractor disappears at 245 μm . *Dashed-dotted lines* show resting membrane potentials for the two cases

3.7 A transition in I_A dynamics can lead to backpropagation failure

In Fig. 4 we showed how the faster reacting, distal form of I_A leads to reduced backpropagation amplitude in models compared to the slower, proximal form. An abrupt transition from the proximal to the distal form at a given location can therefore be expected to cause poor propagation, or possibly no active propagation, distal to the transition location. We test this hypothesis in the model for two locations of the transition from “slow” to fast kinetics (200 and 400 μm , Fig. 5). The traveling wave attractors are almost identical up until 200 μm with only a slight difference due to small differences in resting membrane potential along the dendrite in the two models. With the transition to fast I_A dynamics occurring at 200 μm (gray lines), a step decrease in traveling wave attractor amplitude occurs, followed by its near immediate disappearance. Since this change in channel kinetics is abrupt and not adiabatic as for shifting conductance densities, one does not expect the propagating action potential to follow the underlying steady state, i.e. traveling wave attractor, closely. The transient effect of this non-adiabatic change in channel kinetics is directly observable by comparing solid lines and dashed lines in Fig. 5: the action potential’s amplitude drops off sharply just before 200 μm . The small ledge seen before the second drop off is due to large changes in waveform shape (not shown) near the discontinuity. With the transition to distal I_A dynamics occurring at 400 μm , the traveling wave attractor (dashed black line) disappears and the simulated action potential (solid black line) fails near 400 μm .

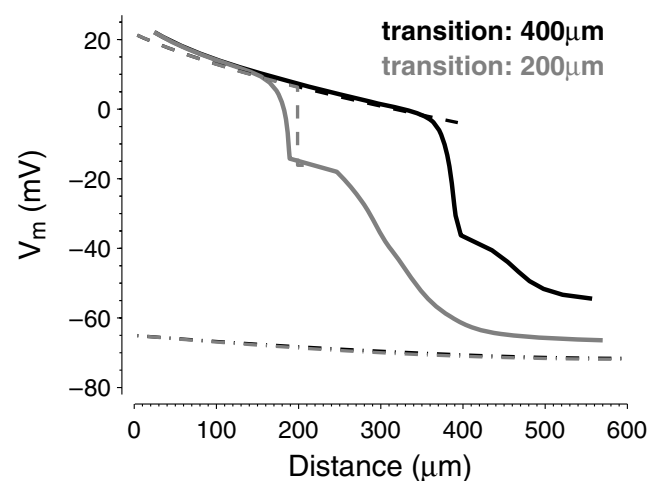


Fig. 5 Transitions in activation properties of I_A strongly influence backpropagation amplitude and backpropagation failure. Same experiment as in Fig. 4 except activation dynamics of I_A abruptly switch from the “slow,” proximal type to the “fast,” distal type at either 200 μm (*gray lines*), or 400 μm (*black lines*)

In Fig. 5, the amplitudes of the simulated backpropagating action potentials drop proximal to the point at which the traveling wave attractor drops off or disappears. This apparently non-causal behavior occurs when the leading edge of the propagating action potential (distal to the peak) propagates in the portion of the dendritic membrane that cannot support the traveling wave. For this reason, the waveform’s peak amplitude can depend on properties distal to the instantaneous peak location. Although step changes in I_A channel kinetics cannot be considered adiabatic, induced transients are mainly restricted to the region immediately surrounding the location of the change in kinetics.

3.8 Propagation of dendritic spikes is affected by changes in I_A dynamics

Dendritic spikes can be generated in distal dendrites of pyramidal cells in region CA1 and elsewhere (Häusser et al. 2000; Golding et al. 2002; Gasparini et al. 2004). Large conductance and especially highly spatio-temporally correlated excitatory inputs landing on small diameter dendrites can cause large membrane depolarizations. Recruitment of dendritic Na^+ or Ca^{2+} voltage-gated conductances can lead to dendritic spikes (Häusser et al. 2000). How these spikes propagate towards the cell soma depends on distributions of voltage-gated channels and channel kinetics, as well as morphology and branch points encountered. In Fig. 6 we show how changes in I_A dynamics, which, as we have demonstrated, strongly affect action potential backpropagation, also strongly affect forward propagation of dendritic spikes.

In the same dendrite model used in Figs. 4 and 5, a brief, large amplitude current pulse (4 nA, 0.5 ms) is applied to the most distal compartment of the dendrite to trigger a dendritic spike. In Fig. 6(a), the amplitude of the forward propagating spike is shown in the same two cases as in Fig. 4. The “slow” (found on proximal dendrites, black lines) and “fast” (found on distal dendrites, light gray lines) types of I_A are incorporated with identical distributions. Dashed lines show the traveling wave attractor amplitudes for the two cases, which are identical to those in Fig. 4. There is a large difference in the amplitude of forward propagation between the two cases. When the slow type of I_A is present on the entire dendrite, the dendritic spike is carried all the way to the soma, where it elicits an action potential. As it propagates towards the soma, its amplitude steadily increases as predicted by the traveling wave attractor. In contrast, when the fast type of I_A is present along the entire dendrite, the dendritic spike fails to propagate and its amplitude quickly decays to zero. This can be explained in terms of the traveling wave attractors. The distal dendrite, where the spike is generated, does not

support a propagating action potential as indicated by the absence of the traveling wave attractor. This situation is different than the case of failing backpropagating action potential, which propagates for a certain distance before failing. Here the dendritic spike is a transient effect of the dendritic stimulation and never propagates as a traveling wave. By the time the spike reaches the portion of the dendrite that exhibits a traveling wave attractor and therefore supports a propagating action potential, its amplitude is severely diminished and is therefore unable to elicit a propagating action potential in the proximal dendrite.

In Figs. 6(b) and (c), the time domain responses to the dendritic current pulse as measured at the soma and stimulation site, respectively, are shown. In addition to the two cases shown in panel a, the two examples from Fig. 5 are also shown in which transitions from proximal to distal I_A dynamics take place at 200 and 400 μm using intermediate shades of gray. At the distal tip (600 μm), there is a small but clear difference in amplitude between the case that successfully forward propagates and the

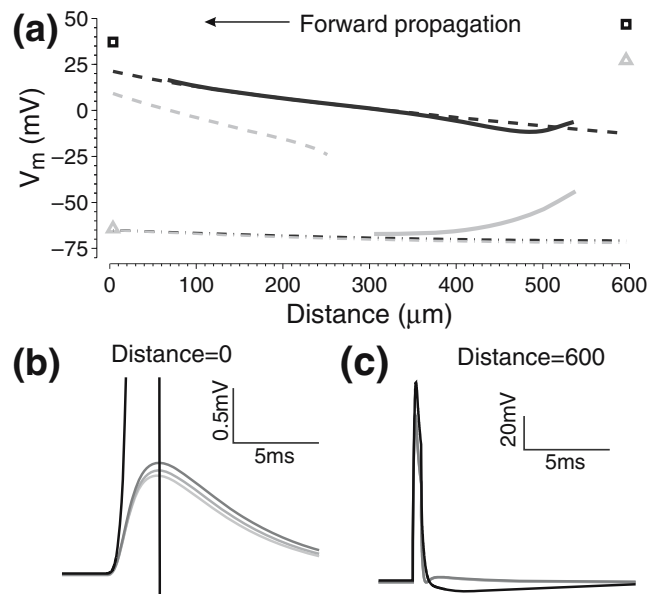


Fig. 6 Forward propagation of dendritic spikes is influenced by activation properties of I_A . (a) Current pulses (4 nA, 0.5 ms) are applied to the most distal dendritic compartment (600 μm) in order to elicit dendritic spikes that travel right to left. Peak amplitudes of the forward propagating spike are shown (solid lines) for the same two cases considered in Fig. 4 (black for “slow” I_A and light gray for “fast” I_A). Open symbols are peak amplitudes of time waveforms at soma and distal tip. Dashed lines are traveling wave attractor amplitudes (identical to Fig. 4). (b) Somatic responses for the two cases shown in panel a (light gray and black lines), along with two additional cases in which I_A dynamics switch from slow to fast at 200 and 400 μm (intermediate gray scale lines). The somatic action potential elicited in the case of “slow,” i.e. proximal I_A activation is clipped. (c) Dendritic spikes recorded at stimulation site. Same format as panel (b)

others, which all overlap very closely. However, this difference is not sufficient to explain the observed results, since use of a larger current pulse cannot rescue forward propagation in the cases shown that fail (data not shown). The voltage responses measured at the soma (distance = 0 μm) are similar (approximately 1.5 mV amplitudes) in all cases except when the slow (proximal) form of I_A is present along the entire dendrite (black lines), which leads to a full amplitude somatic action potential (voltage trace clipped).

When the density of I_A rises unceasingly along the length of the apical dendrites as in Fig. 6, the scenario that forward propagation of distally generated dendritic spikes is only possible when I_A is of the slow form seems likely. While this form of I_A was observed experimentally on the proximal regions of CA1 apical dendrites and not on the distal regions (Hoffman et al. 1997), the kinetics of I_A was shown to be phosphorylation dependent (Hoffman and Johnston 1998). It is therefore possible that under different circumstances with different protein kinase activity in the distal dendrites, I_A might be in the slow form in the distal dendrites thereby permitting the possibility of forward propagation. Since there is some evidence that the I_A conductance density in the distal tuft might drop (Rhodes et al. 2004), it is also necessary to keep in mind the possibility that forward propagation of distally generated dendritic spikes might be possible to some extent if I_A if the conductance is sufficiently reduced. Recall that with reduced channel densities, the fast form of I_A permits propagation (Fig. 4, proximal region).

Finally, it is important to mention that even with channel properties conducive to forward propagation, the extent of forward propagation may be limited by dendritic branching. Branching is especially unfavorable for forward propagating dendritic spikes that are initiated on fine branches and attempt to invade the dendritic arbor compared to back-propagating action potentials. More on this will be discussed after the effects of branching on propagation are presented in detail in the context of backpropagating action potentials. Without conditions (both channel properties and branching) conducive to forward propagation of solitary, distally generated dendritic spikes, successful propagation to the soma may require some form of “cooperativity.” Synaptic inputs may trigger several dendritic spikes on separate branches simultaneously, or synaptic activation may lead to sufficient dendritic depolarization to permit successful forward propagation (Jarsky et al. 2005).

3.9 Contributions of dendritic morphology to backpropagating action potential amplitude

Dendritic morphology, including variations in diameter of dendritic processes, and patterns of branching, shapes electrical signaling properties of neuronal dendrites (Rall

1959; Goldstein and Rall 1974; Mainen and Sejnowski 1996; Vetter et al. 2001). Modeling studies have shown that amplitude of backpropagation can be dramatically different in models that feature different morphologies but identical distribution and properties of ion channels (Vetter et al. 2001). We now reincorporate the originally published, apical dendrite morphology data from a reconstruction of a CA1 pyramidal cell (Migliore et al. 1999). By holding channel properties the same as in the simple cable model, one can compare backpropagation amplitude in the two models. This comparison, with the help of the local traveling wave information, allows one to tease out effects due specifically to dendritic morphology in non-uniform dendrite models.

3.10 Using traveling wave attractors to compute action potential transients in dendrite models with non-uniform channel properties

Cable models with uniform channel properties have a constant steady-state behavior given by the traveling wave attractor. Propagation velocity depends on diameter as given by Eq. (2), while the waveform of the propagating action potential represented by the attractor, plotted as a function of time, is independent of diameter. Branches or abrupt changes in diameter can lead to failure (see Fig. 9 below), or cause transient changes in the waveform (e.g., in amplitude) and permanent propagation delays or advances. In models with uniform channel properties, these amplitude transients and changes in timing can be quantitatively understood as a function of the geometric ratio (GR, Eq. (3) below, Goldstein and Rall 1974) calculated at each branch point or diameter change location (Goldstein and Rall 1974; Manor et al. 1991). The GR is defined as (Rall 1959):

$$\text{GR} = \frac{\sum_j d_j^{3/2}}{d_p^{3/2}}. \quad (3)$$

Diameters of the j daughter branches, d_j , form the numerator with the diameter of the parent branch, d_p , in the denominator. Branch points with $\text{GR} > 1$ cause transient decreases in amplitude, those with $\text{GR} < 1$ cause transient increases in amplitude, while with $\text{GR} = 1$, the amplitude is unaffected (Goldstein and Rall 1974).

In dendritic models with non-uniform membrane properties, quantitatively predicting effects of branching is more difficult, because the steady-state propagation behavior is no longer constant along the dendrite. In cases for which changes in channel properties can be considered adiabatic (e.g., Fig. 3), calculated responses in the absence of branching follow the traveling wave attractor closely. In

these cases, it is possible to calculate the transient amplitude effects of branching by calculating the difference between amplitudes from simulations and amplitudes of traveling wave attractors computed along the dendrites.

3.11 Effects of branching on backpropagation amplitude

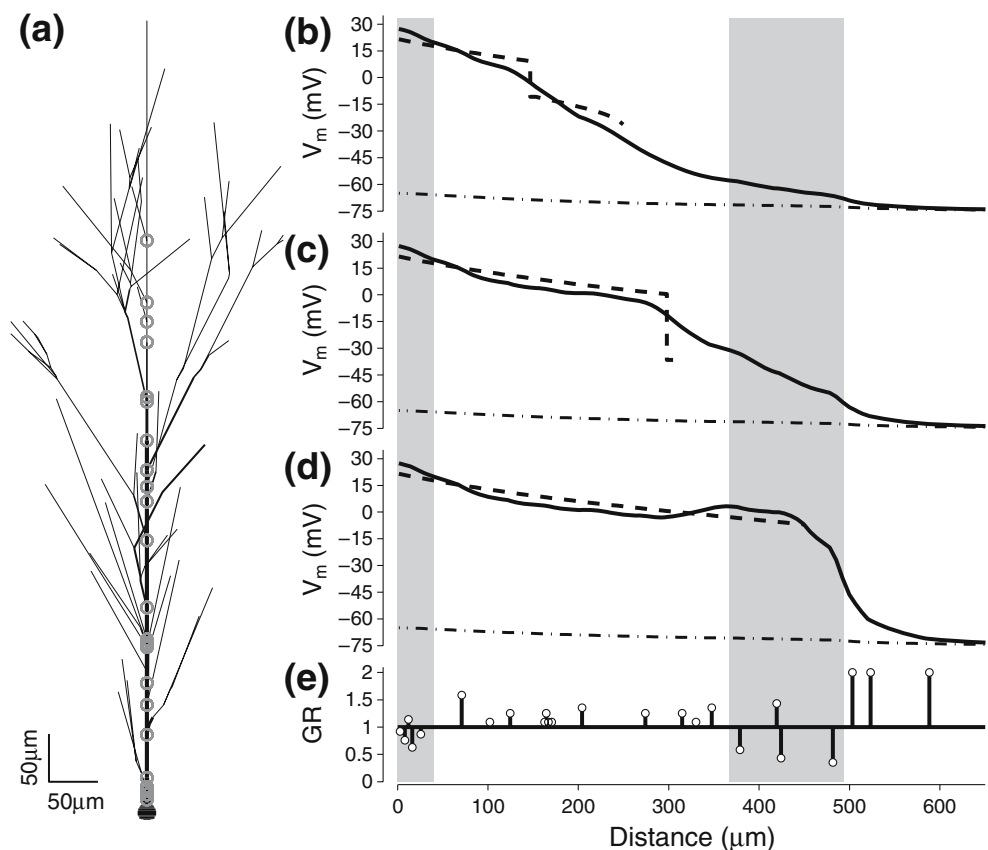
A diagram of the morphologically detailed CA1 pyramidal cell model is shown in Fig. 7(a) (Migliore et al. 1999). In this diagram, angles between sections were chosen randomly, with the exception that the longest series of sections, with the distal tip lying 830 μm from the cell's soma, is plotted on the vertical axis. Backpropagation along this series of sections, which will be referred to as the “principal branch,” is studied here (all branches are studied in Fig. 8). Locations of changes in diameter along with branch point locations are indicated by open circles on the model diagram. Finally, Fig. 7(e) shows the geometric ratio values (GR, Eq. (3)) for each branch.

Somatic action potentials are triggered using brief current pulses as before, and resulting backpropagating action potential amplitude as a function of distance from soma along the principal branch for three cases is shown in Fig. 7(b), (c), and (d), solid lines. In these three cases, the

transition from “proximal” to “distal” I_A dynamics occurs at three different locations (distance=150, 300, and 450 μm in Fig. 7(b), (c), and (d), respectively). The amplitude of the local traveling wave attractors is shown using dashed lines in each of the three cases.

In Fig. 7(b–d), backpropagation amplitude is initially greater than that of the local traveling wave attractor (*leftmost shaded area*). This discrepancy is due mainly to the initial transient caused by the large amplitude somatic action potential. Subsequently, after the action potential passes 65 μm , we observe that its amplitude is less than that predicted by the local traveling wave attractors. In Fig. 7(b), the action potential soon interacts with the location of the transition from slow to fast I_A dynamics. In Figs. 7(c–d), this transition occurs more distally, allowing us to see that the action potential amplitude consistently falls below that of the traveling wave attractor by approximately 4 mV for a distance of roughly 200 μm . Recall that in a branchless model with the same channel properties and distributions (Fig. 5), there is very little amplitude discrepancy. Therefore, we can attribute this 4 mV difference in amplitude to the branches and changes in dendrite diameter encountered along this section of dendrite. Notice that in this region, between 50 and 350 μm , we see a cluster of GR values

Fig. 7 Backpropagation amplitude in a morphologically detailed CA1 pyramidal cell model. **(a)** Diagram illustrating dendrite morphology using published soma and CA1 apical dendrite morphology data. Angles between dendrite sections are chosen from a probability distribution. The longest series of branches is shown as a vertical path. *Open circles* indicate locations of changes in dendrite diameter and branch points. **(b), (c), (d)** Backpropagation amplitude (*solid*), amplitude of underlying traveling wave attractor (*dashed*), and resting potentials (*dashed-dotted*) are shown for three cases. Dynamics of I_A change from “proximal” to “distal” dynamics at locations 150, 300, and 450 μm in panels **(b)**, **(c)**, and **(d)** respectively. **(e)** GR (geometric ratio) values for all branches and changes in diameter along longest, “principal” branch. *Shaded regions* indicate clusters of branches with $\text{GR} < 1$



greater than one (Fig. 7(e)). It has been shown previously that an action potential's amplitude transiently decreases before passing a branch point with a GR value greater than one (Goldstein and Rall 1974). In this section of this model, these effects add up to approximately 4 mV.

When propagation passes 320 μm , the discrepancy between the action potential amplitude and that of the

traveling wave attractor switches from -4 mV to approximately $+5$ mV (Fig. 7(d)), backpropagation has failed by this point in panels (b) and (c). Notice that in this region (shaded) between 350 μm to 500 μm , there is a cluster of GR values less than one. Branches with GR values less than one transiently increase action potential amplitude (Goldstein and Rall 1974). In this region of this model, the effects of

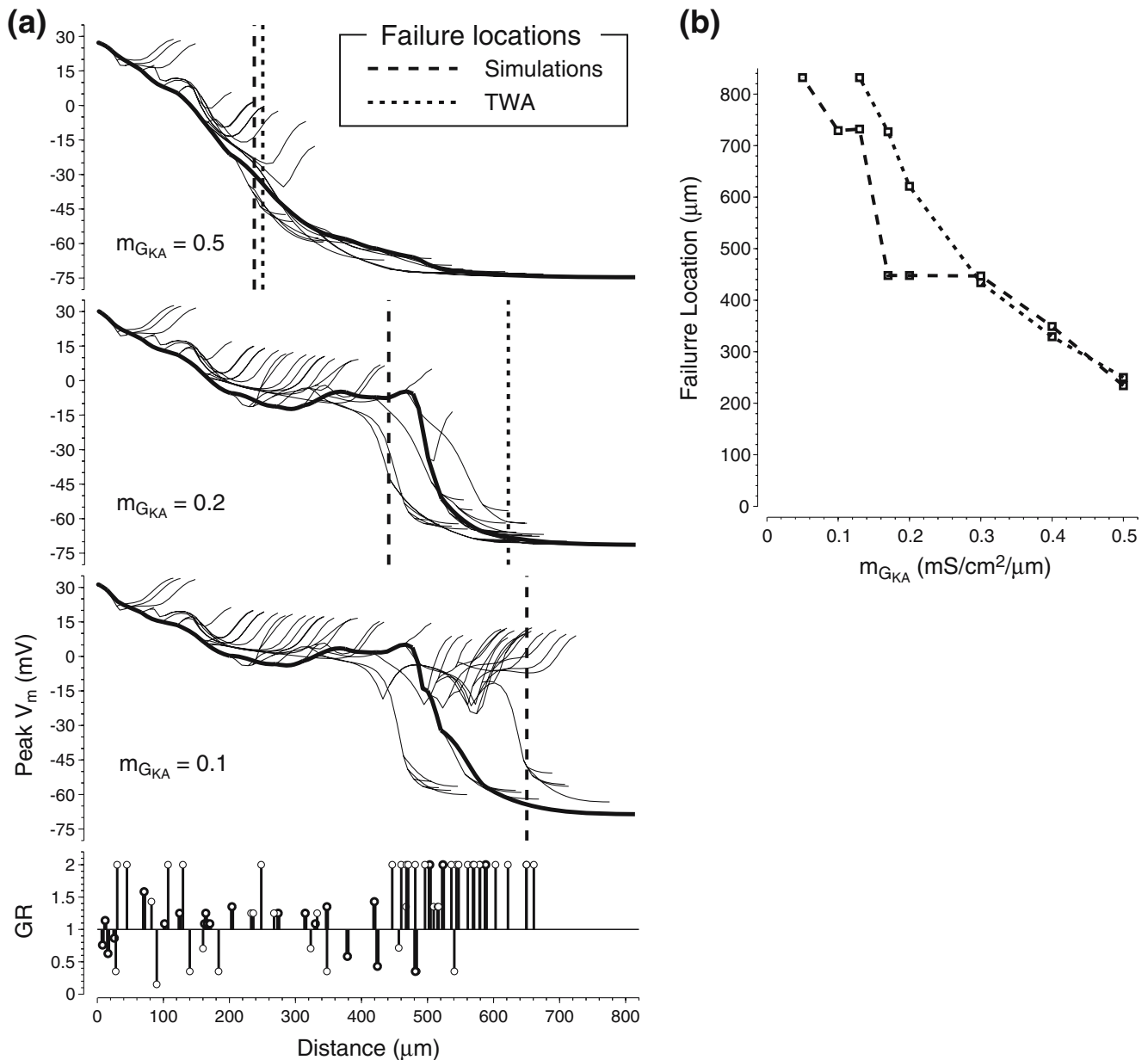


Fig. 8 Action potential propagation failures, without failure of the underlying traveling wave attractor, occur depending on I_A channel properties and distribution, and are due to the influence of dendritic branches. **(a)** Peak amplitudes in all branches of the CA1 pyramidal cell model (see Fig. 7) with three different I_A channel distributions. I_A conductance, g_{KA} , rises linearly with distance (see Fig. 3) with slope $m_{G_{KA}}$ from an initial conductance of $48 \text{ mS}/\text{cm}^2$. Thick black lines are from apical trunk (Fig. 7). Location of the disappearance (failure) of

traveling wave attractor (TWA) along principal branch is indicated by vertical dotted line (no failure in bottom panel). Simulation peak voltage data is pooled, smoothed, and the minimum of the second derivative (see Fig. 3(d)) is used to determine overall location of action potential failure (vertical dashed line). Bottom panel shows GR (geometric ratio) values for all branches. **(b)** Failure locations of TWA (dotted) are plotted along with failures computed from simulation data (dashed) as a function of slope of I_A conductance distribution, $m_{G_{KA}}$

these branches on bAP amplitude accumulate to approximately 5 mV.

3.12 Distal dendritic branches can cause backpropagation failures when intrinsic properties would otherwise support active propagation

The distal portion of the model CA1 dendrites that corresponds to the apical tuft of these cells is comprised of many bifurcations of processes already with small diameters. These bifurcations lead to values of geometric ratio (GR) significantly greater than one. As discussed previously, such branches lead to transient decreases in backpropagating action potential amplitude. If strong enough, these decreases may lead to propagation failure depending on intrinsic membrane excitability properties (Goldstein and Rall 1974). We find that failures do occur in the distal region of the CA1 model due to high-GR branches in regions with a substantial amount of I_A . In these cases, membrane excitability is sufficient to sustain propagation, as indicated by the traveling wave attractor; however, failure is observed in spite of this.

In Fig. 8, the distribution of I_A is varied but the transition from proximal to distal I_A dynamics (varied in Fig. 7) is fixed at 150 μm . Peak membrane potential values for every model compartment are plotted as a function of distance from the soma. Failure locations predicted by location of traveling wave disappearance are compared to failure location found from model simulations (using second derivative data, see Fig. 3(d)) for each of the three I_A channel distributions. Decreasing the slope of the rising I_A conductance density increases the amplitudes of backpropagating action potentials and smoothly delays the point at which the intrinsic dynamics no longer sustain active propagation. However, in simulations, strong effects due to branching between 400 and 600 μm are seen and cause failures in many dendritic branches in this region for a significant range of I_A distributions. When the failure locations predicted by the traveling wave attractor are compared to those found in simulations (Fig. 8(b)), one sees a clear divergence of the two curves plotted as a function of the slope in I_A conductance density. In particular, failures in simulations precede the disappearance of the attractor. Two non-adiabatic changes are possible sources of divergence of simulations and attractors: boundary effects and branches. Because our sealed-end boundaries lead to increases in membrane potential relative to predictions from attractors, as can be seen from the cases in Fig. 8 for which bAPs do not fail, the effects of boundaries would be to reduce the likelihood of failure. In contrast, high-GR branches promote failure of bAPs. Thus, we conclude that the unpredicted failures seen in Fig. 8(b) are caused by dendritic branching.

3.13 Propagation failure at branch points depends on I_A channel properties

Ion channel densities and properties affect action potential amplitude directly. This is evident in branchless models and effects can be predicted by computing the underlying traveling wave attractors (Figs. 1–6). Additionally, action potential transients at branch points with specific parent and daughter branch diameters depend on channel densities and properties (Manor et al. 1991). For example, the same branch point can cause anywhere from negligible effects on action potential amplitude to propagation failure, depending on membrane excitability properties. Spurred by results from Fig. 8, we explored how failure at branch points depends on GR and G_{KA} , the conductance underlying I_A (Fig. 9). As expected, larger values of GR make propagation more difficult; thus, only small values of G_{KA} allow action potentials. The “distal,” faster version of I_A makes the bAP more prone to failure. For G_{KA} approaching the maximal values that permit propagation, the morphological perturbation sufficient to cause propagation failure becomes vanishingly small. For this reason GR values approach 1 near these critical values of G_{KA} (Fig. 9 open symbols).

The propagation failure data in Fig. 9 qualitatively explain why morphology-induced propagation failures are observed in the distal region of the present CA1 model

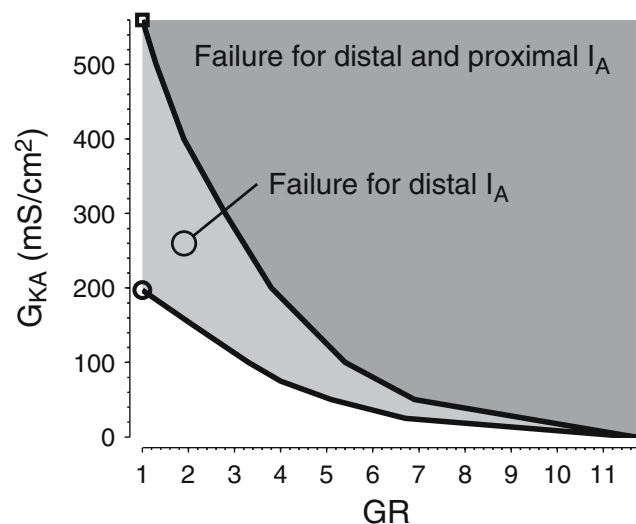


Fig. 9 Propagation failure at branch points depends on I_A conductance density and channel activation properties. *Lines* indicate critical geometric ratio (GR) and I_A conductance density (G_{KA}) pairs that lead to propagation failure in uniform cable models with a single step change in diameter. *Shaded areas* indicate regions of propagation failure for proximal and distal I_A dynamics. A constant, uniform current is adjusted along with G_{KA} to maintain pre-stimulus steady-state membrane potential at -65 mV. Maximal I_A conductance densities for stable propagation are plotted at GR=0 for proximal and distal I_A kinetics (*square and circle*, respectively)

(Fig. 8). Failures at branch points occur when the fast form of I_A is present on the distal dendrites and the channel's conductance density increases with distance at a rate greater than $mG_{KA}=0.18 \text{ mS/cm}^2/\mu\text{m}$ (Fig. 8(b)). Failures cluster around $450 \mu\text{m}$ where GR values at branch points are typically 2 (Fig. 8(a) bottom). At $450 \mu\text{m}$, I_A conductance densities are greater than 130 mS/cm^2 for the range of distributions that lead to failure. These results correspond well with the data for solitary branch points, which cause propagation failure for I_A conductance densities greater than 150 mS/cm^2 when $GR=2$ (Fig. 9).

4 Discussion

In this study we take a closer look at how the transient potassium current I_A affects backpropagation of action potentials and forward propagation of dendritic spikes. We find that the activation dynamics of this current can have an especially large impact on propagation. Distally located channels tend to activate at lower potentials and activate more quickly. These distal channel activation properties can lead to backpropagation failure, similar to that seen experimentally. Also, these properties can make it impossible for distally generated dendritic spikes to reach the soma. Because the activation properties of these channels are modulated by common intracellular second messengers (Hoffman and Johnston 1998), it is possible that the cell is able to tune or alter the propagation behavior of backpropagating action potentials and dendritic spikes for some purpose. Interestingly, activation properties of sodium channels are also subject to modulation by the same second messengers and therefore, these channels can also be expected to play a role in “backpropagation modulation” (Gasparini and Magee 2002; Frick et al. 2004).

We discovered that dendrites can have underlying traveling wave attractors that govern backpropagating action potentials and forward propagating dendritic spikes. We describe how to compute these attractors for any model, morphologically simplified or complex. For cases in which conductance densities change adiabatically, these attractors provide nearly perfect descriptions of simulated behavior. For cases in which parameters change abruptly, the traveling wave attractor typically remains qualitatively useful. Depending on the properties of the dendrite, the underlying attractor can change. Changes in attractor amplitude can predict the actual backpropagation behavior from simulations well, depending on the dendrite's morphology. Also, the underlying traveling wave attractor can disappear, and this disappearance has important consequences for dendritic action potentials. In the absence of a stable traveling wave attractor it is difficult or impossible to

trigger a propagating dendritic spike. Synaptic inputs must be large enough such that the membrane potential crosses threshold at any neighboring region that does support a traveling wave. Also, propagating action potentials that encounter the loss of the traveling wave attractor are likely to fail. The failures we see in models resemble those observed experimentally (Golding et al. 2001). The failure location is typically predicted by the point of attractor disappearance. In cases of branch points with large geometric ratios and large values of G_{KA} , failure can be more prominent than predicted by the attractor (Figs. 8, 9).

Changes in dendritic morphology, including branching and dendritic terminations, cause changes in the propagating action potentials (Goldstein and Rall 1974). Associated changes in action potential amplitude are not reflected by traveling wave attractors since dendritic diameter is only relevant for the attractor's wave speed and not its time domain waveform (Hodgkin and Huxley 1952; Goldstein and Rall 1974; Weiss 1996). The resulting discrepancies between the action potential's amplitude and that of the underlying attractor appear a certain distance before the action potential arrives at the change in dendritic morphology. This distance depends on the spatial extent of the action potential which is approximately equal to (exact for traveling waves in uniform cables) the product of the time domain extent (ex. half width) and the wave speed. Wave speed is proportional to the square root of dendritic diameter in exactly the same way as is the dendrite's electrotonic length (Goldstein and Rall 1974). Therefore, dendrites with large diameter are expected to have large wave speed and spatially extended action potentials. These action potentials can be expected to react well in advance of, and possibly more strongly to, any dendritic branch point or termination they encounter. Given these complexities, it seems that the best way to understand the effects of dendritic morphology in a particular model may be to do as we do in this study: compare propagation in the morphologically complex model of interest with propagation in a surrogate model with branch points or terminations removed.

With the help of traveling wave attractors and morphologically simplified models, we are able to distinguish effects on action potential propagation due to branching and changing dendritic diameter from those due to voltage-gated ion channels in a morphologically complex dendrite model. In the model CA1 pyramidal neuron dendrite, effects due to morphology are clearly visible and depend on whether the dendrite is becoming effectively wider or narrower. Typically, these effects are minor; however, distal dendritic branches in the model we studied have particularly large values of GR and can cause action potential failures in the distal dendrites for a range of I_A channel conductances in this region. These effects can be under-

stood in terms of the interplay between morphology and membrane properties (Fig. 9).

The analysis in this paper focused on the effects of time-invariant parameters, including the spatial distribution of G_{KA} and branch points of a given geometric ratio (GR). Traveling-wave-attractor-based analysis could be extended to more complex cases including time-varying inputs, assuming that such inputs could be approximated as adiabatic (e.g., broadly distributed in space and stationary in time).

Excitatory synapses in the distal dendritic region likely follow different learning rules than those in more proximal regions if backpropagation failure is indeed prevalent. Recent experiments in neocortical pyramidal cells demonstrate that responses to spike-timing-dependent plasticity protocols are crucially sensitive on backpropagation (Sjöström and Häusser 2006). We speculate that similar mechanisms are operating in CA1 pyramidal cells, along with more clearly established dependence of CA1 plasticity on local dendritic spikes (Golding et al. 2002). The behavior of bAPs and dendritic spikes in distal regions depends strongly on both channel density and the phosphorylation-determined kinetics of I_A (Hoffman and Johnston 1998). For this reason, it is important to make difficult experimental measurements of channel densities and kinetics (or phosphorylation states) in order to understand the rules of plasticity of proximal and distal synapses more deeply.

Acknowledgements The authors would like to thank: Georgi Medvedev (Drexel University) and Eugene Wayne (Boston University) for early, stimulating input; Bard Ermentrout (University of Pittsburgh) for technical help with XPPAUT; and Jonathan Bettencourt, Kyle Lillis, and Theoden Netoff (NDL, Boston University) for feedback and help editing the final manuscript.

References

- Acker, C. D., Kopell, N., & White, J. A. (2003). Synchronization of strongly coupled excitatory neurons: Relating network behavior to biophysics. *Journal of Computational Neuroscience*, *15*, 71–90.
- Bi, G. Q., & Poo, M. M. (1998). Synaptic modifications in cultured hippocampal neurons: Dependence on spike timing, synaptic strength, and postsynaptic cell type. *Journal of Neuroscience*, *18*, 10464–10472.
- Dayan P., Abbott LF (2001) *Theoretical neuroscience: Computational and mathematical modeling of neural systems*, (p. 220). Cambridge: MIT Press.
- Ermentrout, B. (2002). *Simulating, analyzing, and animating dynamical systems*. Philadelphia, PA: SIAM.
- Frick, A., Magee, J., & Johnston, D. (2004). LTP is accompanied by an enhanced local excitability of pyramidal neuron dendrites. *Nature Neuroscience*, *7*, 126–135.
- Froemke, R. C., Poo, M. M., & Dan, Y. (2005). Spike-timing-dependent synaptic plasticity depends on dendritic location. *Nature*, *434*, 221–225.
- Gasparini, S., & Magee, J. C. (2002). Phosphorylation-dependent differences in the activation properties of distal and proximal dendritic Na^+ channels in rat CA1 hippocampal neurons. *Journal of Physiology*, *541*, 665–672.
- Gasparini, S., Migliore, M., & Magee, J. C. (2004). On the initiation and propagation of dendritic spikes in CA1 pyramidal neurons. *Journal of Neuroscience*, *24*, 11046–11056.
- Golding, N. L., Kath, W. L., & Spruston, N. (2001). Dichotomy of action-potential backpropagation in CA1 pyramidal neuron dendrites. *Journal of Neurophysiology*, *86*, 2998–3010.
- Golding, N. L., Staff, N. P., & Spruston, N. (2002). Dendritic spikes as a mechanism for cooperative long-term potentiation. *Nature*, *418*, 326–331.
- Goldstein, S. S., & Rall, W. (1974). Changes of action potential shape and velocity for changing core conductor geometry. *Biophysical Journal*, *14*, 731–757.
- Gulledge, A. T., Kampa, B. M., & Stuart, G. J. (2005). Synaptic integration in dendritic trees. *Journal of Neurobiology*, *64*, 75–90.
- Häusser, M., Spruston, N., & Stuart, G. J. (2000). Diversity and dynamics of dendritic signaling. *Science*, *290*, 739–744.
- Hodgkin, A. L., & Huxley, A. F. (1952). A quantitative description of membrane current and its application to conduction and excitation in nerve. *Journal of Physiology*, *117*, 500–544.
- Hoffman, D. A., & Johnston, D. (1998). Downregulation of transient K^+ channels in dendrites of hippocampal CA1 pyramidal neurons by activation of PKA and PKC. *Journal of Neuroscience*, *18*, 3521–3528.
- Hoffman, D. A., Magee, J. C., Colbert, C. M., & Johnston, D. (1997). K^+ channel regulation of signal propagation in dendrites of hippocampal pyramidal neurons. *Nature*, *387*, 869–875.
- Jarsky, T., Roxin, A., Kath, W. L., & Spruston, N. (2005). Conditional dendritic spike propagation following distal synaptic activation of hippocampal CA1 pyramidal neurons. *Nature Neuroscience*, *8*, 1667–1676.
- Johnston, D., Christie, B. R., Frick, A., Gray, R., Hoffman, D. A., Schexnayder, L. K., et al. (2003). Active dendrites, potassium channels and synaptic plasticity. *Philosophical Transactions of the Royal Society of London. Series B, Biological Sciences*, *358*, 667–674.
- Johnston, D., Hoffman, D. A., Colbert, C. M., & Magee, J. C. (1999). Regulation of back-propagating action potentials in hippocampal neurons. *Current Opinion in Neurobiology*, *9*, 288–292.
- Magee, J. C., & Johnston, D. (1997). A synaptically controlled, associative signal for Hebbian plasticity in hippocampal neurons. *Science*, *275*, 209–213.
- Mainen, Z. F., & Sejnowski, T. J. (1996). Influence of dendritic structure on firing pattern in model neocortical neurons. *Nature*, *382*, 363–366.
- Manor, Y., Koch, C., & Segev, I. (1991). Effect of geometrical irregularities on propagation delay in axonal trees. *Biophysical Journal*, *60*, 1424–1437.
- Markram, H., Lubke, J., Frotscher, M., & Sakmann, B. (1997). Regulation of synaptic efficacy by coincidence of postsynaptic APs and EPSPs. *Science*, *275*, 213–215.
- Migliore, M., Hoffman, D. A., Magee, J. C., & Johnston, D. (1999). Role of an A-type K^+ conductance in the back-propagation of action potentials in the dendrites of hippocampal pyramidal neurons. *Journal of Computational Neuroscience*, *7*, 5–15.
- Rall, W. (1959). Branching dendritic trees and motoneuron membrane resistivity. *Experimental Neurology*, *1*, 491–527.
- Rhodes, K. J., Carroll, K. I., Sung, M. A., Doliveira, L. C., Monaghan, M. M., Burke, S. L., et al. (2004). KChIPs and $Kv4$ alpha subunits as integral components of A-type potassium channels in mammalian brain. *Journal of Neuroscience*, *24*, 7903–7915.
- Sjöström, P. J., & Häusser, M. (2006). A cooperative switch determines the sign of synaptic plasticity in distal dendrites of neocortical pyramidal neurons. *Neuron*, *51*, 227–238.

- Spruston, N., Schiller, Y., Stuart, G., & Sakmann, B. (1995). Activity-dependent action potential invasion and calcium influx into hippocampal CA1 dendrites. *Science*, *268*, 297–300.
- Stuart, G. J., & Häusser, M. (2001). Dendritic coincidence detection of EPSPs and action potentials. *Nature Neuroscience*, *4*, 63–71.
- Stuart, G. J., & Sakmann, B. (1994). Active propagation of somatic action potentials into neocortical pyramidal cell dendrites. *Nature*, *367*, 69–72.
- Vetter, P., Roth, A., & Häusser, M. (2001). Propagation of action potentials in dendrites depends on dendritic morphology. *Journal of Neurophysiology*, *85*, 926–937.
- Weiss, T. F. (1996). *Cellular biophysics*. Cambridge, MA: MIT Press.